Molecular Phylogenetics and Evolution 81 (2014) 258–270

Contents lists available at ScienceDirect

Molecular Phylogenetics and Evolution

journal homepage: www.elsevier.com/locate/ympev

Phylogenetic position of the bee genera *Ancyla* and *Tarsalia* (Hymenoptera: Apidae): A remarkable base compositional bias and an early Paleogene geodispersal from North America to the Old World

Christophe J. Praz [a,*], Laurence Packer [b]

[a] Institute of Biology, University of Neuchatel, Emile-Argand 11, 2000 Neuchatel, Switzerland
[b] Department of Biology, York University, 4700 Keele St., Toronto, ON M3J 1P3, Canada

ARTICLE INFO

Article history:
Received 7 May 2014
Revised 5 September 2014
Accepted 9 September 2014
Available online 18 September 2014

Keywords:
Non-stationarity
Biogeography
Eucerini
Ancylaini
North Atlantic Land Bridge
Stepping stone method

ABSTRACT

We address the phylogenetic position of the bee genera *Tarsalia* and *Ancyla* (currently forming the tribe Ancylaini) on the basis of morphological, molecular and combined data. We assembled a matrix of 309 morphological characters and 5246 aligned nucleotide positions from six nuclear genes (28S, EF-1a, wingless, POL2, LW-Rhodopsin, NAK). In addition to both constituent genera of Ancylaini, we include all three subtribes of the Eucerini as well as a large number of other tribes from the "eucerine line". The morphological data suggest *Ancyla* to be sister to *Tarsalia* + Eucerini and analyses of the entire molecular dataset suggest *Tarsalia* to be sister to *Ancyla* + Eucerini. However, analyses of the combined dataset suggests the Ancylaini to be monophyletic. We address possible bias within the molecular data and show that the base composition of two markers (EF-1a and NAK) is significantly heterogeneous among taxa and that this heterogeneity is strong enough to overcome the phylogenetic signal from the other markers. Analyses of a molecular matrix where the heterogeneous partitions have been RY-recoded yield trees that are better resolved and have higher nodal support values than those recovered in analyses of the non-recoded matrix, and strongly suggest the Ancylaini to be a monophyletic sister group to the Eucerini. A dated phylogeny and ancestral range reconstructions suggest that the common ancestor of the Ancylaini reached the Old World from the New World most probably via the Thulean Land Bridge in a time window between 69 and 47 mya, a period that includes the Early Eocene Climatic Optimum. No further exchanges between the New World and the Old World are implied by our data until the period between 22 mya and 13.9 mya. These more recent faunal exchanges probably involved geodispersal over the Bering Land Bridge by less thermophilic lineages.

1. Introduction

The higher-level classification of the bees has been, for the most part, remarkably stable since it was developed by Michener in 1944 (Danforth et al., 2013; Gonzalez et al., 2013; Michener, 2007); the monophyly of most families, subfamilies and tribes is well established and has been confirmed by numerous phylogenetic studies using morphological (e.g., Alexander and Michener, 1995; Gonzalez et al., 2012; Roig-Alsina and Michener, 1993; Straka and Bogusch, 2007) or molecular data (Almeida and Danforth, 2009; Cardinal et al., 2010; Cardinal and Danforth, 2013; Danforth et al., 2004, 2006; Litman et al., 2011). Within families, however, the tribal assignment and the phylogenetic position of some genera remain controversial, especially within the large and diverse family Apidae (Cardinal et al., 2010; Payne, 2014). In particular, the phylogenetic position of the genera *Ancyla* and *Tarsalia* has long been unsettled. These two genera are found in warm, Mediterranean to tropical regions of the Old World. The nine species of *Ancyla* are found from Northern Africa to the Middle East, in xeric areas with mean annual temperature (MAT) above 18 °C (Ascher and Pickering, 2014). They fly in high summer and all species may be oligoleges on the plant family Apiaceae (Straka and Rozen, 2012). The seven known species of *Tarsalia* are distributed from India to the xeric Mediterranean regions of South-eastern Europe (Ascher and Pickering, 2014). They also fly in high summer and are restricted to areas with MAT above 16 °C; the Palaearctic species may be oligoleges on Asteraceae (C. Praz, pers. observation). The presence of these genera in the Old World is puzzling from a biogeographic perspective, as they lack any close relatives

* Corresponding author.
E-mail address: christophe.praz@unine.ch (C.J. Praz).

http://dx.doi.org/10.1016/j.ympev.2014.09.003
1055-7903/

in the Eastern Hemisphere (Cardinal et al., 2010; Roig-Alsina and Michener, 1993; Silveira, 1993a, 1995), but rather belong to a group that has its center of diversity in megathermal parts of the New World.

At present, *Ancyla* and *Tarsalia* are united as a tribe, the Ancylaini (Michener, 2007). The systematic position of this tribe has been problematic partly because *Ancyla* has a mouthpart morphology more typical of short-tongued bees (Silveira, 1993b; herein Fig. S1a), a feature most likely associated with specialization to the shallow flowers of the Apiaceae. Conversely, *Tarsalia* has typical long-tongued bee mouthparts (Fig. S1b). The putative relationship between these two genera has ranged from them being considered as congeneric (Warncke, 1979) to being "not closely related" (Baker, 1998); further confusing assessment of their position within the phylogeny of bees.

The phylogenetic placement of the Ancylaini has been examined in a few studies. Roig-Alsina and Michener (1993) presented analyses based upon up to 131 characters from adults (as well as additional analyses including larval characters separately or combined with adult data); they included *Tarsalia* but not *Ancyla*. The results were variable but generally suggested that *Tarsalia* was the sister group to the Eucerini. Silveira (1993a, 1995) added *Ancyla* to Roig-Alsina and Michener's (1993) data. The results similarly varied with the details of the analysis performed, but the author suggested that Ancylaini and Exomalopsini were both monophyletic and sister taxa to one another within the "eucerine line" (i.e. including the Eucerini, Emphorini and Tapinotaspidini). Baker (1998) considered the phylogenetic position of *Tarsalia* in an analysis of 63 morphological characters. He included all described species of *Tarsalia* but had an idiosyncratic and perfunctory sample of other genera. *Ancyla holtzi* Friese was used to root the tree thereby precluding monophyly of the Anclyaini.

The first extensive molecular phylogenetic research pertinent to the placement of the Ancylaini is Cardinal et al. (2010) who found *Ancyla* to be sister to the Eucerini with high support values (*Tarsalia* was not included). The Cardinal et al. (2010) molecular dataset was combined with a morphological matrix (mostly from Roig-Alsina and Michener, 1993 and Straka and Bogusch, 2007) and reanalyzed using parsimony methods by Payne (2014), also without *Tarsalia*. Payne (2014) found *Ancyla* to be sister to the Eucerini for all nine transformation cost regimes employed.

Any investigation of the relationship of the Ancylaini to the Eucerini should include both *Ancyla* and *Tarsalia* as well as taxa representing the earliest diverging branches of eucerine evolution and other groups within the "eucerine line". The monotypic, Chilean genus *Eucerinoda* is traditionally considered to be the sister group to the remaining Eucerini, as it is the only eucerine with the paraglossa shorter than the first labial palpomere (see also the results of Roig-Alsina and Michener, 1993). It had been considered as possibly extinct until rediscovered in 2008 (Vivallo, 2010). Similarly monotypic but restricted to Argentina, *Canephorula* is considered as sister to the remaining Eucerini (*Eucerinoda* excepted) on the basis of its possessing a simply recurved gradulus to the second sternum of females; all other eucerini (except *Eucerinoda*) have the gradulus birecurved (Michener, 2007). These seemingly important morphological differences between the two genera and between them and the remaining Eucerini has led to the tribe being classified in three subtribes: Eucerinodina, Canephorulina and Eucerina respectively (Michener, 2007). The only studies of apine phylogeny to include all three subtribes were those of Roig-Alsina and Michener (1993) and Silveira (1993a) and the results of both studies varied depending upon the details of the dataset analysed. No molecular study has included *Tarsalia*, *Eucerinoda* or *Canephorula*.

The purpose of the present study is to investigate the relationships among *Ancyla*, *Tarsalia*, the Eucerini and associated bee lineages using both morphological and molecular data with taxon sampling that includes *Eucerinoda* and *Canephorula*, as well as representative members of the Eucerina. As our analyses of the morphological, molecular and combined datasets actually yield all of the three possible branching patterns between *Ancyla*, *Tarsalia* and the Eucerini, we carefully examine possible biases in our molecular dataset. We show that base composition of some partitions is strongly heterogeneous among taxa (base compositional non-stationarity), potentially introducing bias in phylogenetic inference. We demonstrate that RY-recoding of the heterogeneous partitions, a technique developed to remove base composition bias in the analysis of mammalian mitochondrial genomes (Phillips and Penny, 2003), dramatically influences the inferred topology. Under such a recoding regime, all analyses of the molecular dataset yield highly resolved and supported trees that were different from those obtained under standard analyses of the molecular dataset. Lastly, we use a dated phylogeny to infer a biogeographical scenario for the eucerine line, with particular reference to the dating of the exchanges between western and eastern hemispheres.

2. Materials and methods

2.1. Choice of taxa

We downloaded sequences of all species belonging to the following tribes from Genbank: Ancylaini, Emphorini, Eucerini, Exomalopsini and Tapinotaspidini, mainly from the Cardinal et al. (2010) dataset (Table S1). We did not include the genera *Arrhysoceble* (Tapinotaspidini) and *Meliphilopsis* (Emphorini) because both sexes were not available for morphological analyses, and included only one representative of *Ancyloscelis* (Emphorini) and of *Anthophorula* (Exomalopsini). We included the following species among the outgroups for parsimony analyses: *Ctenoplectra albolimbata* Magretti (Ctenoplectrini), *Tetrapedia maura* Cresson (Tetrapediini), *Centris atripes* Mocsáry (Centridini), *Pachymelus peringueyi* (Friese) (Anthophorini) and *Manuelia gayatina* (Spinola) (Manuelini), using the latter to root the trees (as we also did in model-based analyses) as it is the sole member of the subfamily Xylocopinae included. We augmented this dataset with *Tarsalia*, *Eucerinoda*, *Canephorula* and two species of *Alloscirtetica*. We thus provide sequence data for the subtribes Eucerinodina and Canephorulina as well as *Tarsalia* and *Alloscirtetica* for the first time. We included two species of *Alloscirtetica* because this genus was previously divided into subgenera that differ with respect to some seemingly important morphological characters and also because initial (and final) analyses suggested that it may be sister to the remaining genera of Eucerina. Our dataset thus includes 17 eucerine taxa, two species of *Ancyla* (of which only one was coded for morphology), one species of *Tarsalia*, 11 species representing the other tribes of the eucerine line, and 5 outgroup species representing other apid tribes (Table S1). In several cases, it was not possible to include the same species within a genus for both morphological and molecular analyses. For this reason, terminals in the combined analysis are only labeled by generic name.

2.2. Morphology

The characters used by Roig-Alsina and Michener (1993) and Silveira (1995) were augmented by detailed study of the external and internal morphology of the taxa listed in Table S2. Only the non-genitalic internal morphology of *Tarsalia* and some characters for female *Svastrina* were not assessed, due to scarcity of specimens, although for *Tarsalia* the tentorial characters were taken directly from Roig-Alsina and Michener (1993). The characters used in earlier papers were often reformulated, or discarded, in

light of the variability found among the different taxa we investigate. A full list of characters, supplementary methodological details for morphological procedures as well as the morphological matrix are provided in the Appendix.

2.3. Phylogenetic analysis of the morphological dataset

The morphological data matrix was entered into Winclada (Nixon, 2004), which served as the interface to spawn to the program NONA (Goloboff, 1999), where preliminary analyses were performed using the Parsimony Ratchet (Nixon, 1999). The results were verified through driven searches in TNT (Goloboff et al., 2008) with the seed set to 0 (ie, the clock), with ratchet, tree drift and tree fusing all with default options and 5 initial sequences added. "Find min. length" was set to 100. Successive approximations character weighting (Farris, 1969; Carpenter, 1988) was used to assess the stability of the resulting tree(s) using the "run.rewt run" script available with TNT and the rescaled consistency index as the weighting factor. Support for the various nodes in the most parsimonious tree from the raw data was assessed using both traditional bootstrap (hereafter BS) and symmetric resampling routines in TNT with 1000 replications (Goloboff et al., 2003). GC values are the percentage of times that a particular resolution was found at a node minus the number of times that the next most frequent resolution in which that grouping did not occur.

2.4. Molecular data

2.4.1. Gene fragments

Tarsalia persica (Warncke) was collected in ethanol in the field; for other taxa, we used pinned specimens collected between one and 10 years prior to analysis. We sequenced the five nuclear, protein-coding genes used in Cardinal et al. (2010), namely elongation factor 1-alpha (F2 paralog; see Danforth and Ji, 1998; hereafter EF-1a), LW-Rhodopsin (Opsin 1 of Spaethe and Briscoe, 2004; hereafter Opsin), wingless (wnt1 paralog), RNA-polymerase II (hereafter Pol II), and sodium potassium adenosine triphosphatase (hereafter NAK), as well as the ribosomal gene 28S; in contrast to Cardinal et al. (2010), we did not include 18S, which is more conserved and phylogenetically less informative than 28S (see comments in Cardinal et al. (2010): Supplementary material, partitioning of data). We used the primers cited in Cardinal et al. (2010) for PCR reactions, with some exceptions that are mentioned in the Appendix.

2.4.2. Lab protocols

Full lab protocols can be found in Praz et al. (2008). DNA was isolated using phenol-chloroform extractions; PCR reactions were performed with Hotstart GoTaq polymerase (Promega) in a Biometra T1 thermocycler; PCR products were purified enzymatically using a mix of the enzymes exonuclease I (Fermentas) and FastAP thermosensitive alkaline phosphatase (Fermentas) and sequenced in both directions with the primers used in the original amplification using BigDye terminator technology (Applied Biosystems) in 12 µl reaction volumes (0.5 µl of BigDye, 2.5 µl of BigDye buffer, 0.17 µl primer 10 M and 2–8 µl purified PCR product). Big Dye products were purified with Sephadex (GE Healthcare Life Sciences) and analyzed on an ABI-3130 DNA sequencer at the Genetic Diversity Center, ETH Zürich.

2.5. Sequence assembly and alignment

The chromatograms were trimmed and assembled using the software Sequencher 4.7 for Macintosh (Gene Codes Corp.). All sequences were aligned in Mafft with default parameters (Katoh et al., 2002) and the alignments were corrected visually in MacClade 4.08 for Macintosh OSX (Maddison and Maddison, 2005). Reading frame and intron/exon boundaries were determined by comparison with published sequences for *Apis mellifera*. Only EF-1a and Opsin have introns, which were removed in MacClade prior to analysis: they were difficult to align unambiguously and preliminary single-gene analyses with the few conserved fragments included did not result in better resolved trees than in analyses without introns. The coding sequences were converted to amino acid sequences to ensure that the correct reading frame had been found. Each protein-coding gene was trimmed to start at nucleotide position one and end at position three. The ribosomal gene 28S was aligned in Mafft and entirely corrected visually in MacClade; a few ambiguous regions were excluded from the analyses. In several cases, we coded as missing data short sequences in outgroup taxa (see above: choice of taxa) to facilitate unambiguous alignment within the eucerine line.

2.6. Data exploration

Ratios of synonymous to non-synonymous substitutions were computed for each protein-coding gene with the method of Yang and Nielsen (2000), implemented in PAMLX (Xu and Yang, 2013). To explore the saturation of the phylogenetic information for the third nucleotide position, we used two approaches. First, we use the index of substitution saturation developed by Xia et al. (2003) and implemented in DAMBE (Xia, 2013; Xia and Lemey, 2009) to test for saturation at the third nucleotide position in each protein-coding gene; second, we followed Niehuis et al. (2012) and plotted uncorrected distances against corrected distances (under the Tamura-Nei substitution model) for the third nucleotide position of each protein-coding gene. Pairwise distances were computed in MEGA 5.2.2 (Tamura et al., 2011). Deviation from a straight line indicates saturation due to multiple substitutions at the same site. Heterogeneity (non-stationarity) in base composition across taxa was explored for each codon position of the protein-coding genes, and for 28S using the chi-square test implemented in a test version of PAUP (Swofford, 2002) for OSX kindly made available by D. Swofford. In case of significant heterogeneity, the partition was degenerated to RY (all T and C were transformed to Y and all A and G to R) (Phillips and Penny, 2003) and tested again with PAUP.

2.7. Phylogenetic analyses of the molecular dataset and total evidence analyses

Each analysis (Maximum parsimony, Maximum likelihood and Bayesian analyses; hereafter MP, ML and BA, respectively) was conducted with: a. the full molecular dataset, b. the full dataset to the exclusion of EF-1a (including this gene resulted in a substantial proportion of missing data; see the Appendix), and c. the full dataset with heterogeneous partitions recoded to RY. For each of them, we conducted analyses with and without *Canephorula*, as this taxon could be sequenced for one gene only. We also ran MP, ML and BA analyses of the combined molecular + morphology matrix.

Parsimony analyses were performed with TNT using the same options as outlined above for morphological analysis (without successive weighting). ML analyses were conducted in RAxML 7.2.8 (Stamatakis et al., 2005). We first analyzed each gene individually, dividing each dataset into three partitions for the protein-coding genes (one partition for each codon position). Then, the six genes were concatenated and the resulting matrix was divided into four (entire dataset) or five partitions (RY-recoded dataset): three partitions corresponding to each of the three codon positions (except the RY-recoded nucleotides), a fourth partition comprising all nucleotide sites of 28S, and a separate partition for the RY-recoded third nucleotide position, if applicable. We applied a GTR + G

model to each partition; we did not fit both a proportion of invariant sites (+I) and a gamma distribution (+G) to the same partition. To analyse the partition containing the RY-recoded nucleotides, we used two approaches. First, we applied a GTR + G model to this partition in spite of overparameterization, and second, we recoded R and Y as 0 and 1 and enforced a binary model to the resulting binary partition. Both approaches yielded nearly identical trees. Bootstrap support values were calculated based on 1000 replicates. All consensus trees were visualized in FigTree v.1.3.1.1 (Rambaut, 2012). We also explored ML analyses of the entire dataset partitioned by gene (thus with six partitions), as well as a more complex partitioning regime with 6 partitions (1: NAK nt1, POL2 nt1, wingless nt1; 2: NAK nt2, POL2 nt2; 3: NAK nt3, Opsin nt3; 4: EF-1a nt3, POL2 nt3; 5: 28S, EF-1a nt1 and nt2, Opsin nt1, Opsin nt2, wingless nt2; 6: wingless nt3), as indicated by the software PartitionFinder (Lanfear et al., 2012). In combined molecular + morphology analyses, the morphology was added as a distinct, numerical partition (''MULTI'') analyzed using the MK model (enforced by the ''-K MK'' command). In the analyses with RY-recoded partition and morphology, the RY-recoded partition was analyzed with a GTR + G, as the MK-model, which is not adequate for molecular data, can only be enforced for all binary partitions in RAXML.

Bayesian analyses of the concatenated dataset were performed in MrBayes v.3.1.2 (Huelsenbeck and Ronquist, 2001; Ronquist and Huelsenbeck, 2003). We applied a GTR + G model to each partition (three partitions corresponding to each of the three codon positions, one partition for 28S and one partition for the RY-recoded third nucleotide position, if applicable). The RY-recoded partition was recoded as 0 and 1 and modeled with the default settings for binary data in MrBayes; as this binary partition includes invariable sites, unlike morphological datasets, we made sure that the parameter ''coding'' was set to ''all''. The morphology partition was added as an additional, numerical partition, also modeled with the default settings, except that the parameter ''coding'' was set to ''variable''. For each analysis, we ran two independent runs of ten million generations each. As convergence diagnostics, we used the standard deviation of split frequencies (a value below 0.01 was already reached after 50,000 generations), the Potential scale reduction factor (all values were equal to 1.000), and the minimal estimated sample size (values for all parameters were above 5000). In addition, Tracer v.1.6 (Rambaut et al., 2014) was used to determine the stationarity of each parameter and to assess an appropriate burnin. As every parameter of the GTR model reached stationarity, we did not explore the use of more simple models (e.g., HKY). We used TreeAnnotator (Drummond et al., 2012) to eliminate the burnin and to calculate consensus trees from both independent runs. Trees were visualized in FigTree v1.3.1. Lastly, we compared the marginal likelihood estimates of alternative topologies differing in the position of *Ancyla* and *Tarsalia* using the stepping stone sampling approach implemented in MrBayes. We constrained three alternative topologies in analyses of the entire molecular dataset, with and without RY recoding (without morphology, with *Canephorula* excluded): *Tarsalia* sister to *Ancyla* + Eucerini; *Ancyla* sister to *Tarsalia* + Eucerini; and *Ancyla* + *Tarsalia* sister to Eucerini. We ran an initial run of one million generations to reach stationarity, followed by 30 steps of 1 million generations (alpha = 0.4), thus in total 31 million generations, sampling every 1000 generations and discarding 25% of the samples at each step. Convergence was reached in most steps, with only a few values of split frequencies around 0.012 in steps 20–25. Further details on the stepping stone analyses are provided in the Appendix.

2.8. Dating analysis and biogeography

Only one fossil is known from the eucerine line (Michez et al., 2011), and its generic or even tribal assignment requires confirmation. Therefore, we used BEAST 1.8 (Drummond et al., 2012) and two calibration points taken from Cardinal and Danforth (2013) to produce a dated phylogeny. Cardinal and Danforth (2013) provide estimated ages for important bee clades according to three analyses (their Table S6); we selected here values of the third analysis, which is the one with the youngest age estimates. We placed a normal prior (mean 100.0, standard deviation 5.0) on the age of the root of our tree (parameter treeModel.rootHeight), corresponding to the 95% interval for the age of the family Apidae, and a normal prior (mean 82.0, standard deviation 5.5) to age the node uniting all members of the eucerine line (Cardinal and Danforth, 2013). We chose our best model and partitioning regime for this BEAST analysis (see below). Each partition had its own substitution model, but the clock model and the tree estimation were linked across partitions. A rate multiplier (compound parameter) was applied to each partition by modifying the xml file. We used an uncorrelated lognormal relaxed clock, set the tree prior to ''Yule process'' and used a random starting tree. The analysis was run for 100 million generations and trace files for all parameters were examined with Tracer v. 1.6 (Rambaut et al., 2014); the lowest effective sample size for any parameter was above 1000. We ran the same analysis twice independently, yielding identical results. A maximum clade credibility tree was calculated and annotated using TreeAnnotator (Drummond et al., 2012) after removing an appropriate burn-in, and visualized in FigTree.

Probabilistic inference of ancestral range was performed in Lagrange (Ree and Smith, 2008) and BioGeoBEARS (Matzke, 2013) in R (R core team, 2014). As input tree, we used the consensus tree from the BEAST analysis after removal (using the ''drop.tip'' function of the ape package in R: Paradis et al., 2004) of five terminals representing the tribes Anthophorini, Ctenoplectrini, Tetrapediini, Centridini and Manuelini. We ensured that phylogenetic uncertainty had no impact on the inferred biogeographic scenario by running Lagrange with three alternative tree topologies, corresponding to the only three nodes which had posterior probability below 0.99 in the Beast analysis. Alternative topologies affected neither the state reconstruction at important nodes (root of the tree, ancestor of Ancylaini) nor the inferred biogeographic scenario (number of faunal exchanges between the different biogeographic regions). Likewise, although our sampling of eucerine genera is not exhaustive, in addition to all the major groupings of New World clades, we include members of all Old World genera with the exception of the monotypic and rare *Notolonia* which is likely an autapomorphic species of *Eucera* or *Tetraloniella*.

Because we focused on early-diverging Eucerini as well as on *Tarsalia* and *Ancyla*, which are all absent from the Afrotropical and Oriental zones (with the exception of some species of *Tarsalia* found in India, both of which are derived taxa according to Baker's (1998) phylogeny for the genus), we implemented a simple model with only three geographic areas recognized: South America (A), North America (B) and Old World (C). The maximal number of areas that could be occupied by one terminal was set to two. We excluded the unrealistic range AC (South America and Old World). In Lagrange, this was done using the online Lagrange Configurator; in BiogeoBears, this was achieved by loading a restricted list of possible ranges using the command ''BioGeoBEARS_run_object$states_list =list_restricted''. Both Lagrange and BioGeoBears give exactly the same results as they implement the same DEC (geodispersal-extinction-cladogenesis) model. In addition to a simple, unconstrained analysis, we used two different approaches to compare the likelihood score of alternative biogeographic scenarios: in Lagrange, we ran an analysis where geodispersal between North America and the Old World was not possible before 30 mya by implementing two different geodispersal matrices (100 mya–30 mya; 30 mya–0 mya). In BioGeoBears, we ran one analysis where the ancestor of the Ancylaini was constrained to be absent from the Old World (using the commands ''fixnodes'' and ''fixlikes''). Both

constrained models specifically test the hypothesis that the Ancylaini originated in the New World and that both genera (*Ancyla*, *Tarsalia*) became extinct in the New World after having reached the Old World independently.

3. Results

3.1. Morphological

Three hundred and nine morphological characters were scored (see the Appendix for an annotated list of characters and character states). This dataset gave one most parsimonious tree with a length of 2109 steps, CI of 34 and RI of 59 (Fig. 1; see Fig. S2 for the same tree with character changes mapped onto it). This tree was, with the exception of the position of *Diadasia*, stable to successive approximations character weighting with weights stabilizing after two iterations. In the equal weights tree, *Diadasia* is sister to (*Diadasina* + *Alepidosceles*), whereas in the weighted result it is sister to (*Melitoma* + *Ptilothrix*).

Groups that were found to be monophyletic with strong (GC $\geqslant$ 96%, BS $\geqslant$ 92%) support are (Fig. 1; Table 1): Tapinotaspidini, Emphorini (minus *Ancyloscelis*), Exomalopsini, *Ancyla* + (*Tarsalia* + Eucerini), Eucerini minus *Eucerinoda* (ie Canephorulina + Eucerina) and the Eucerina (ie the traditional Eucerini minus both *Eucerinoda* and *Canephorula*).

Monophyly of the traditional Eucerini and the sister relationship of *Tarsalia* to the traditional Eucerini were less strongly supported (GC 63% and BS 54% for the former and 44 and 50 respectively for the latter; Table 1). Relationships among the groups Tapinotaspidini, Exomalopsini, Emphorini and Eucerini as well as the grouping of *Tetrapedia* with the Tapinotaspidini and *Ancyloscelis* with the remaining Emphorini were all less strongly supported.

Table S3 and Fig. S1 show the unambiguous synapomorphies for the nodes of particular interest and the associated plesiomorphic state(s) and provides comments on the characters.

3.2. Molecular

3.2.1. Dataset

After trimming and removal of the introns and the ambiguous regions of 28S, the concatenated matrix consists of 5246 aligned nucleotide positions (NAK: 1461; POL2: 840; wingless: 456; opsin: 501; EF-1a: 549; 28S: 1439). The molecular dataset was complete for *Tarsalia persica* and for *Alloscirtetica chilena*; EF-1a was entirely missing for *Eucerinoda* and *Alloscirtetica paraguayensis* (Friese), as well as for all eucerine species (except *Melissodes* and *Florilegus*) previously included in the dataset (Cardinal et al., 2010); for *Canephorula*, only 28S could be amplified due to the degraded DNA (Table S1).

Opsin was the gene with the highest ratio of non-synonymous to synonymous mutations (0.109), followed by EF-1a (0.020), NAK and wingless (both 0.014) and POL2 (0.004). Results from DAMBE were comparable for each gene; they all suggest "substantial saturation" (Iss.cAsym not significantly larger than ISS; see Xia and Lemey, 2009) for the third nucleotide position assuming an asymmetrical topology, but little saturation if a symmetrical topology is assumed. The plot of corrected versus uncorrected distances for the third nucleotide (Fig. S3a) position strongly deviates from a straight line beyond a value of approximately 0.2 (corrected distance), and the deviance becomes particularly severe around corrected distances of 0.4, where approximately one fourth of all substitutions are "invisible" (Fig. S3a). When plotted separately,

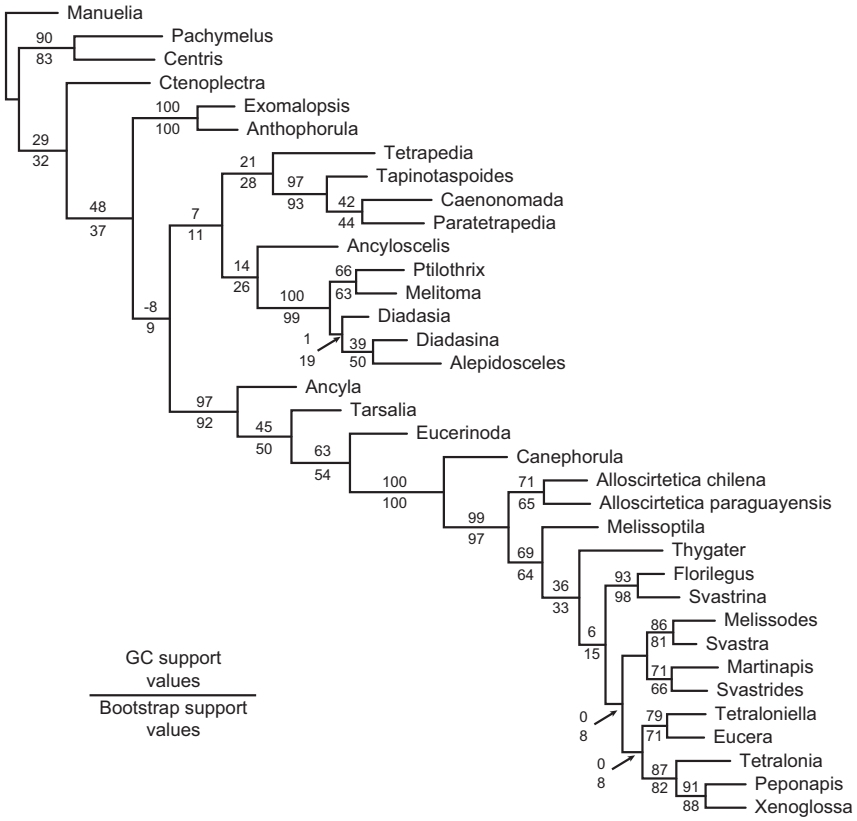

Fig. 1. Single most parsimonious tree found in maximum parsimony analysis of the morphological dataset. GC support values (see text for an explanation) are indicated above the branches, bootstrap support values (BS) below (see Fig. S2 for this tree with character state changes mapped onto it).

Table 1
Support values for important nodes in the different analyses of our dataset. "RY-recoded" indicates analyses where the partitions with heterogenous base composition (third nucleotide positions of EF-1a and NAK) have been recoded to R and Y.

	Morphology	DNA					
	MP BS/GC	Entire dataset MP BS/ML BS/Bayesian PP		Without EF-1a MP BS/ML BS/Bayesian PP		RY-recoded MP BS/ML BS/Bayesian PP	
		With *Canephorula*	Without *Canephorula*	With *Canephorula*	Without *Canephorula*	With *Canephorula*	Without *Canephorula*
Tarsalia + *Ancyla* + Eucerini	>92/>96	83/79/0.87	100/99/1.0	78/57/1.0	95/67/1.0	82/65/0.98	96/82/0.98
Tarsalia + *Ancyla* (Ancylaini)	–/–	–/–/–	–/–/–	–/93/1.0	–/93/1.0	96/99/1.0	96/99/1.0
Ancyla + Eucerini	–/–	72/55/0.83	100/69/0.98	<50/–/–	82/–/–	–/–/–	–/–/–
Tarsalia + Eucerini	51/45	–/–/–	–/–/–	–/–/–	–/–/–	–/–/–	–/–/–
Eucerini	58/61	71/78/0.87	98/100/1.0	60/80/1.0	97/99/1.0	71/79/1.0	94/97/1.0
Canephorulina + Eucerina	>92/>96	<50/58/0.81	na	–/56/0.85	na	–/55/0.78	na
Eucerina	>92/>96	76/88/0.97	100/100/1.0	80/95/0.98	100/100/1.0	78/93/0.99	100/100/1.0
Eucerina minus *Alloscirtetica*	69/64	69/98/1.0	72/100/1.0	85/99/1.0	80/100/1.0	99/99/1.0	100/100/1.0

	DNA + morphology					
	Entire dataset MP BS/ML BS/Bayesian PP		without EF-1a MP BS/ML BS/Bayesian PP		RY-recoded MP BS/ML BS/Bayesian PP	
	With *Canephorula*	Without *Canephorula*	With *Canephorula*	Without *Canephorula*	With *Canephorula*	Without *Canephorula*
Tarsalia + *Ancyla* + Eucerini	100/100/1.0	100/100/1.0	100/100/1.0	100/100/1.0	100/100/1.0	100/100/1.0
Tarsalia + *Ancyla* (Ancylaini)	–/73/0.92	–/67/0.81	–/79/1.0	–/75/1.0	88/74/1.0	83/67/1.0
Ancyla + Eucerini	98/–/–	97/–/–	<50/–/–	54/–/–	–/–/–	–/–/–
Tarsalia + Eucerini	–/–/–	–/–/–	–/–/–	–/–/–	–/–/–	–/–/–
Eucerini	100/100/1.0	99/100/1.0	99/99/1.0	99/98/1.0	97/98/1.0	94/99/1.0
Canephorulina + Eucerina	100/100/1.0	na	100/100/1.0	na	100/100/1.0	na
Eucerina	96/100/1.0	100/100/1.0	98/100/1.0	100/100/1.0	100/100/1.0	100/100/1.0
Eucerina minus *Alloscirtetica*	86/100/1.0	90/100/1.0	81/100/1.0	88/100/1.0	100/100/1.0	100/100/1.0

plots of distances for the third nucleotide position of all five protein-coding genes were very similar (data not shown), and, for example, plots for Opsin (a fast-evolving gene with comparatively high ratio of non-synonymous to synonymous mutations) or EF-1a (a slow-evolving gene) were virtually identical (Fig. S3b).

Lastly, two genes exhibited heterogeneous base composition, EF-1a and NAK. In both cases, it was the third nucleotide position that accounted for this heterogeneity: position 1 and 2 were homogenous when tested separately. For the third position of EF-1a, the Eucerini and *Ancyla* were strongly GC-biased (67.8–81.4% GC for the Eucerini and 73.8% for both species of *Ancyla*), where all other terminals had balanced frequencies or were AT-rich (Fig. 2a). A similar trend was seen in the third position of NAK, although in this case the GC-ratio for *Ancyla* was intermediary between the ratios of *Tarsalia* and of the Eucerini (Fig. 2b). RY-recoding of these partitions removed the bias in both cases.

3.2.2. Phylogenetic analyses

ML analyses of each gene individually yielded the following results: *Ancyla* and *Tarsalia* formed a monophyletic group in analyses of 28S alone (BS 85%), Opsin (BS < 50%) and Pol2 (BS 72%). Analyses of 28S alone recovered a monophyletic Eucerini (BS 51%), but Opsin and Pol2 alone did not. *Tarsalia* was sister to *Ancyla* + Eucerini in analyses of EF-1a alone (BS 76% for the node supporting *Tarsalia* + *Ancyla* + Eucerini; and 100% for that supporting *Ancyla* + Eucerini). In analyses of NAK alone, *Ancyla* was sister to Eucerini (BS 61% for the node supporting *Ancyla* + Eucerini and 63% for the node supporting Eucerini), and the position of *Tarsalia* was not resolved. In analyses of wingless alone, both *Tarsalia* and *Ancyla* were in a large polytomy with the other tribes of the eucerine line.

MP analysis of the entire molecular dataset gave 4 most parsimonious trees with lengths of 5972, CI of 38 and RI of 50. The strict consensus of these had *Tarsalia*, *Ancyla*, *Eucerinoda*, *Canephorula*, *Alloscirtetica* and the remaining Eucerini forming an unresolved polytomy. All four of the original trees had *Tarsalia* as sister to the Eucerini plus *Ancyla* except for one in which *Tarsalia* + *Canephorula* formed a monophyletic group sister to the remaining Eucerini plus *Ancyla*. Removing *Canephorula* from the dataset resulted in a single most parsimonious tree with a length of 5936, CI of 38 and RI of 51. This tree was very similar to the morphology-based tree except that *Tarsalia* was sister to *Ancyla* + Eucerini and *Thygater* and *Melissoptila* formed a sister group that itself was sister to *Svastra* and *Melissodes*. The nodes uniting *Ancyla* with the Eucerini, all Eucerini and Eucerini minus *Eucerinoda* all had high support (Table 1). RY recoding of this dataset both with and without *Canephorula* gave the same pattern as above for the nodes of interest except that the Ancylaini formed a monophyletic sister group to the Eucerini with high support (Table 1). Support values for the relevant nodes in MP analyses of various subsets of the molecular data are shown in Table 1.

ML-analyses of the entire, non-recoded molecular matrix partitioned by codon-position weakly suggested that *Tarsalia* was the sister group to *Ancyla* + Eucerini (Fig. S4; Table 1). The three lineages formed a rather well supported monophyletic group (BS 79%), but the sister relationship between *Ancyla* and Eucerini was poorly supported (BS 55%; the other 45% of the trees showed *Ancyla* + *Tarsalia* to form a monophyletic group). In ML analyses of the entire dataset partitioned by gene, support for the sister relationship between *Ancyla* and the Eucerini was somewhat higher (74%), while under the best-fit partitioning scheme suggested by PartitionFinder, support for the same relationship was below 50%. In the analysis of the matrix partitioned by codon position, the Eucerini was recovered as a well-supported monophyletic group, and within this tribe, *Eucerinoda* was the first branch, then *Canephorula* and then *Alloscirtetica* (Fig. S4; BS values in Table 1). The Tapinotaspidiini and Exomalopsini were monophyletic, but not the Emphorini: the genus *Ancyloscelis* (constituting the subtribe Ancyloscelina; Michener, 2007) was sister to Emphorini + Tapinotaspidiini. Majority-rules consensus trees of the Bayesian analyses were identical for the above-mentioned nodes (Fig. S4; Table 1). *Tarsalia*, *Ancyla* and Eucerini formed a weakly-supported monophyletic group (PP 0.87), within which *Tarsalia* was the first branch; *Ancyla* was sister to all Eucerini (PP 0.83), which formed a monophyletic group (PP 0.87).

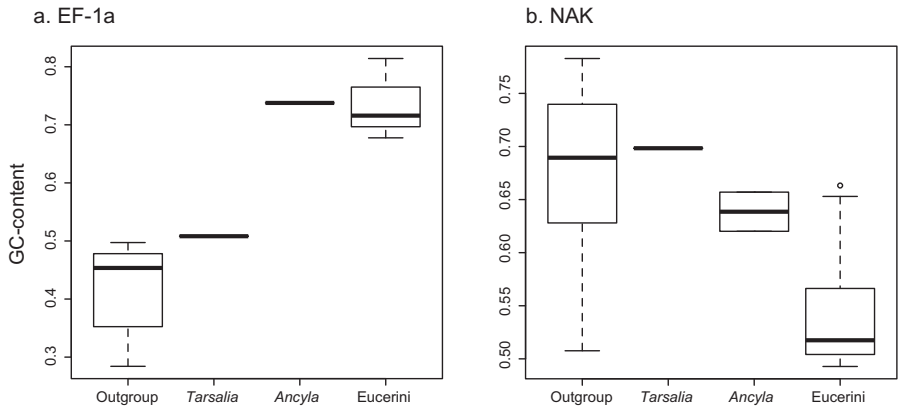

Fig. 2. Boxplots showing the GC-content of the third nucleotide positions of EF-1a (a) and NAK (b) for *Tarsalia*, *Ancyla*, the Eucerini, and all other terminals included in this study, labeled here for simplicity as "outgroup".

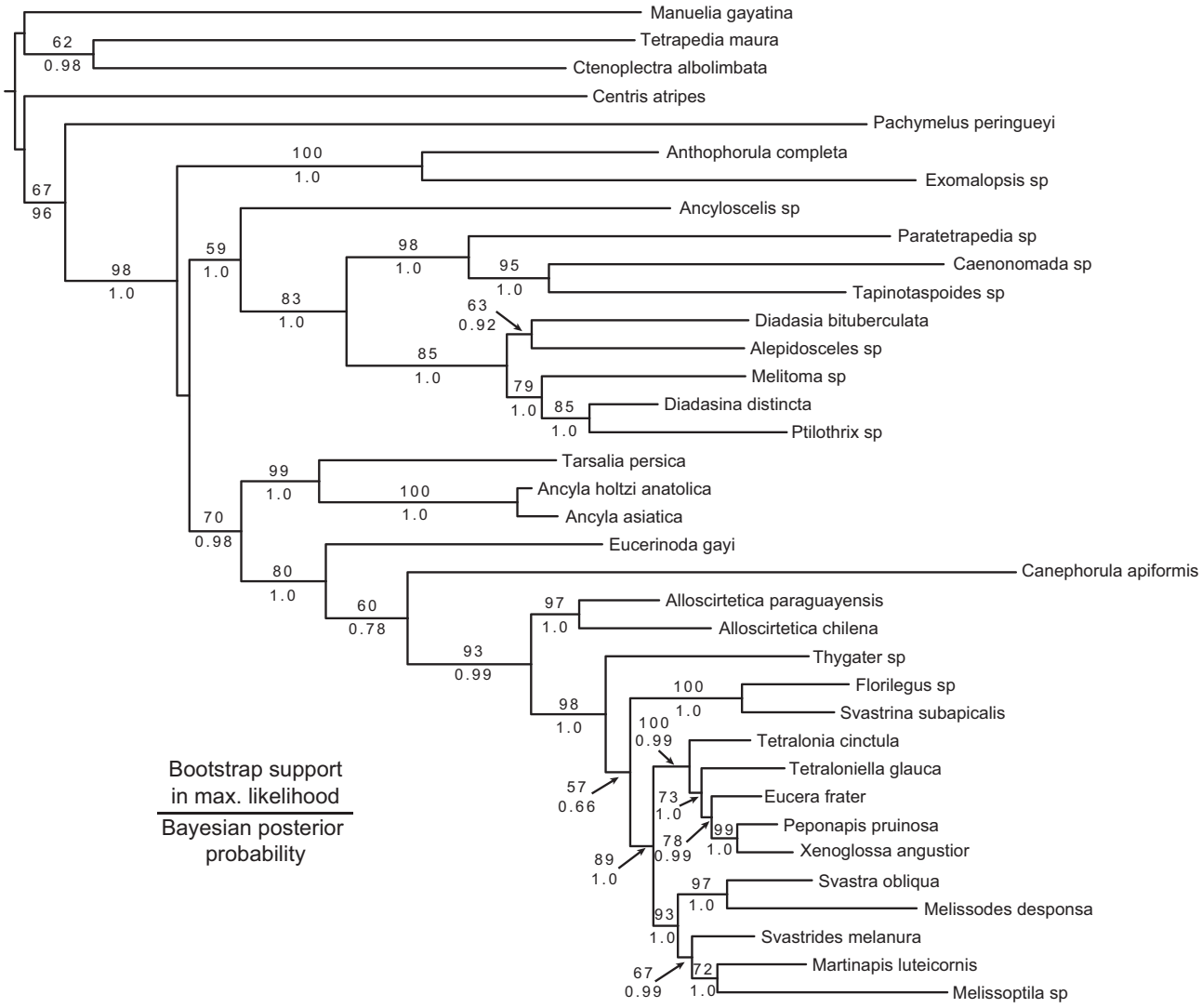

Fig. 3. Best tree found in maximum likelihood analyses of the concatenated (six-gene) molecular dataset with partitions with heterogeneous base composition (third nucleotide positions of NAK and EF-1a) recoded to RY and analysed as an additional, numerical (binary) partition; branch support values above the branches are bootstrap values based on 1000 bootstrap replicates in maximum likelihood analyses of the entire matrix divided into 5 partitions (nt1, nt2, nt3, 28S, RY-recoded nt3); values below the branches are posterior probability values in Bayesian analyses under the same partitioning regime.

In model-based methods (ML and BA), the exclusion of *Canephorula* did not alter the topology, although the support values for the relationships among *Ancyla*, *Tarsalia* and the Eucerini were higher in analyses without this taxon (Table 1). When EF-1a was excluded from the molecular dataset, ML and Bayesian analyses recovered a well-supported, monophyletic Ancylaini (BS 93%, PP

1.0; Table 1). Similarly, ML and Bayesian analyses where the heterogeneous partitions (third nucleotide positions of EF-1a and NAK) were recoded to RY strongly supported a monophyletic Ancylaini, with very high support values (BS 99%, PP 1.0; Fig. 3; Table 1). Trees under such recoding regimes were highly resolved and had higher support values than in the standard (non-recoded) analysis: of 30 nodes within the eucerine line, 29 had BS values above 50% in ML analyses (26 in the standard analysis) and 25 had values above 70% (21 in the standard analysis).

Marginal likelihood values for the different topologies suggest the following results: analyses of the entire, non-recoded dataset (without *Canephorula*) where *Tarsalia* was constrained to be sister to *Ancyla* + Eucerini were slightly favoured over analyses where the Ancylaini were constrained to be monophyletic (difference in log likelihood 4.7 units), but strongly favoured over analyses where *Ancyla* was constrained to be sister to Eucerini + *Tarsalia* (26 units). In analyses of the RY-recoded matrix, analyses where the Ancylaini were constrained to be monophyletic were strongly favoured over either alternative topology (18.9 and 18.2 units).

3.3. Combined analyses

ML and BA analyses of the molecular and morphological datasets combined into one matrix supported a monophyletic Ancylaini sister to Eucerini with moderate support values (BS 73%, PP 0.93; Table 1). In contrast, MP analyses of the combined dataset still placed *Tarsalia* as the sister group to *Ancyla* and Eucerini, with high support (BS 98%; Table 1). All combined analyses also provide strong support for monophyly of the Eucerini, for *Canephorula* plus the Eucerina and for the Eucerina (Table 1). Adding the morphology to the partly RY-recoded matrix did not alter the topology presented in Fig. 4 (whether *Canephorula* was included or excluded) other than for some of the more derived groupings within the Eucerina, but resulted in different support values for some nodes (Table 1).

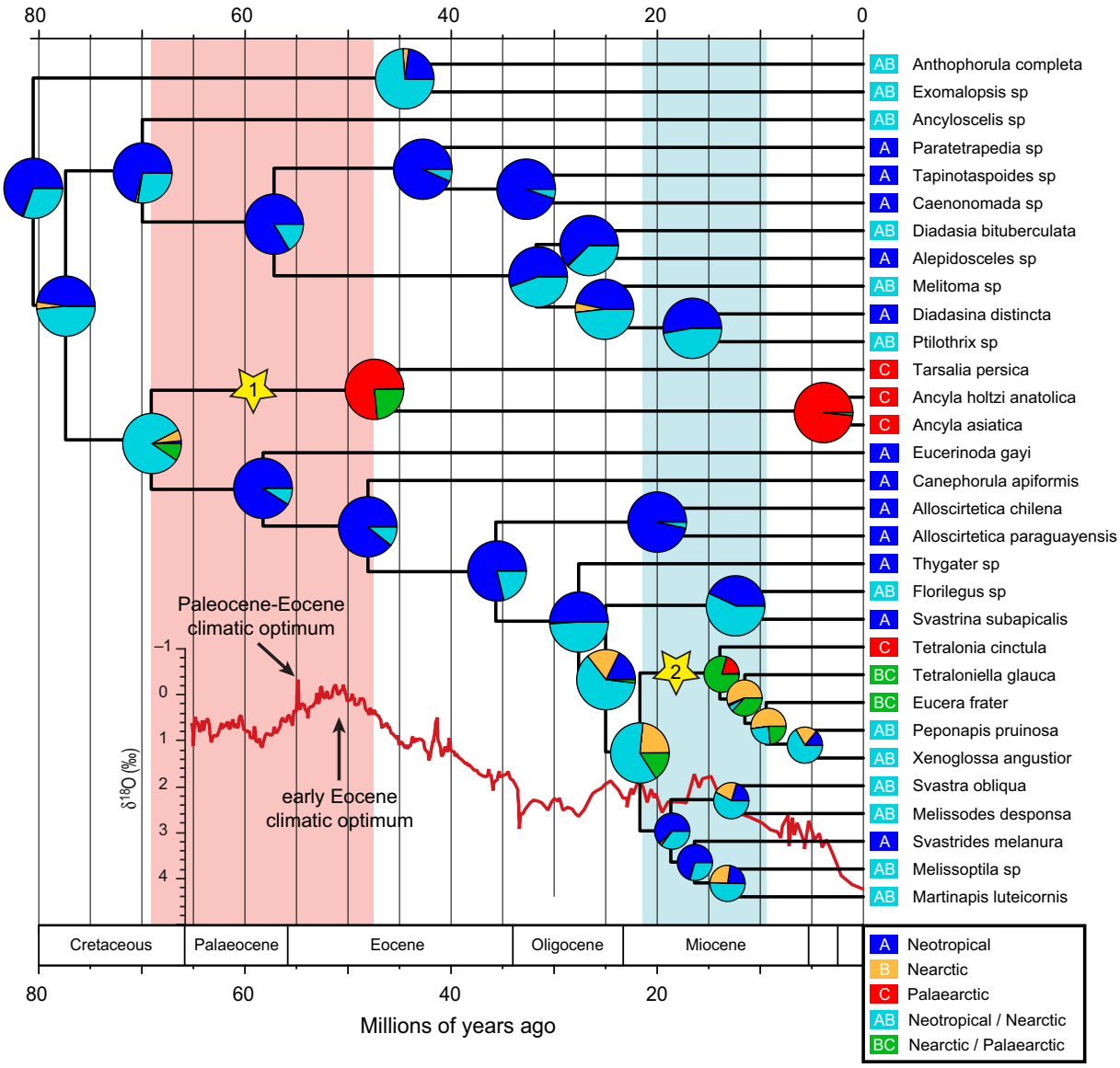

Fig. 4. Ancestral range reconstructions and biogeographical scenario for the Eucerine line based on BioGeoBears analyses. The tree is a maximum clade credibility tree based on the Beast analysis of the molecular dataset with partitions with heterogeneous base composition recoded to RY. The pie-charts show the probability of each reconstruction for each node. Our data suggest two distinct periods of exchanges between the Eastern and Western Hemispheres: one paleogene (69–47 mya, indicated by the red shaded area) geodispersal (star 1) from North America to the Palaearctic, possibly through the Thulean Land Bridge; and several Miocene (23–13.9 mya, indicated by the blue shaded area) exchanges (star 2), possibly over the Bering Land Bridge. The red curve (reproduced from Zachos et al., 2008) indicates climatic evolution between 65 mya and the present, based on deep-sea benthic foraminiferal oxygen-isotope ratios ($\delta^{18}O$).

3.4. Divergence dating analysis and biogeography

We used the complete molecular matrix with heterogeneous partitions (third nucleotide positions of EF-1a and NAK) recoded to RY for the divergence dating analysis in Beast. The resulting majority-rule consensus tree (Fig. 4) is identical to that found in the Bayesian analysis performed in MrBayes. The age of the node uniting the Ancylaini and Eucerini was estimated as 69 mya (95% confidence interval 57–81 my), and the node uniting the two genera of Ancylaini 47 mya (27–65 my). The unconstrained ancestral range reconstructions using BioGeoBears (Fig. 4) and Lagrange were identical in their parameter values and likelihood scores. However, the ancestral states are calculated under the global likelihood model in BioGeoBears (Fig. 4), while in LAGRANGE ancestral states are conditional on fixing each possible state at each node (Matzke, 2013); ancestral range reconstructions were therefore not exactly identical between both approaches, although very similar. Both approaches suggest the same biogeographical scenario (values taken from the Lagrange analysis; see Fig. 4 for the inferred range in the BioGeoBears analysis; inferred ranges with likelihood values over 2 log-units compared to the most likely state are not presented here, as a difference of two likelihood unit suggests significant difference (Pagel, 1999)). The range of the most recent common ancestor (MRCA) of the eucerine line was either South America (−lnL 45.8) or distributed over both South and North America (−lnL between 47.3 and 48.0); the MRCA of the Eucerini and Ancylaini (69 mya) was inferred to be distributed over both South and North America (−lnL 45.5); the range of the MRCA of the Eucerini was reconstructed as being South America, and the MRCA of the Ancylaini (47 mya) was either restricted to the Old World (−lnL 46.5) or present over both North America and the Old World (−lnL 46.6). These ancestral range reconstructions strongly indicate one range expansion, or "geodispersal" (*sensu* Upchurch, 2008) event from the New World to the Old World between 69 and 47 mya. No further exchanges between the New World and the Old World are implied by our data until the period between 22 mya and 13.9 mya, along the branch leading to the clade containing *Tetralonia*, *Tetraloniella*, *Eucera*, *Peponapis* and *Xenoglossa* (*Tetralonia* is restricted to the Old World, *Tetraloniella* and *Eucera* are Holarctic, and *Peponapis* and *Xenoglossa* are restricted to the New World; Michener, 2007). Alternative scenarios implying a North American MRCA of the Ancylaini and two independent range expansion events in *Tarsalia* and *Ancyla* had significantly worse likelihood values (Lagrange analyses: unconstrained analysis −lnL = 45.21; analysis preventing faunal exchanges between the New World and the Old World before 30 mya −lnL = 49.92; BioGeoBears: unconstrained analysis 45.2; analysis where the MRCA of the Ancylaini was forced to be absent from the Old World 49.1).

4. Discussion

Our analyses of the morphological dataset and of the complete molecular dataset yield conflicting results. Although with moderate support, the morphological dataset suggests *Ancyla* to be the sister group to *Tarsalia* + Eucerini, whereas the molecular dataset suggests *Tarsalia* to be the sister group to *Ancyla* + Eucerini. The branching pattern between *Tarsalia*, *Ancyla* and the Eucerini represents a classic situation of long branches juxtaposed with short internodes (Lockhart and Cameron, 2001). In fact the results of our analyses differ only in the placement of the root at the base of Eucerini + *Tarsalia* + *Ancyla*. Both morphology and molecules are prone to different types of systematic error. Convergent evolution (homoplasy) represents the most serious challenge in morphological datasets, and the best way to minimize this bias is to include more characters. With more than 300 characters, our morphological dataset is among the largest such matrices ever compiled for bees and adding new non-molecular characters would be challenging especially considering that immature stages, nest architecture as well as most details on behavior are largely unknown for *Tarsalia, Eucerinoda* and *Alloscirtetica*. Nucleotide data, on the other hand, are prone to well-known biases due to the limited number of character states. Several issues can be distinguished: missing data, saturation of phylogenetic information, rate heterogeneity among sites, and base compositional bias among taxa. Here we briefly discuss the extent to which these may apply to our dataset.

4.1. Missing data

The effect of missing data on phylogenetic reconstruction remains debated (Crawley and Hilu, 2012; Hovmöller et al., 2013; Lemmon et al., 2009; Roure et al., 2012; Wiens and Morill, 2011; Wiens and Tiu, 2012). Our molecular dataset includes two distinct sources of missing data. First, *Canephorula* could be sequenced for one gene only (28S). The position of *Canephorula* within the Eucerini was well established in our analysis of the morphological dataset (sister to all other Eucerini except *Eucerinoda*); most analyses of the molecular dataset also recovered *Canephorula* as sister to all Eucerini except *Eucerinoda*, although the support was moderate (Table 1). Interestingly, the inclusion of *Canephorula* influenced the support values for the node supporting *Ancyla* + Eucerini in analyses of the entire dataset: support for this node was substantially lower if *Canephorula* was included (BS 72%, BS 55% and PP 0.83 in MP, ML and Bayesian analyses; Table 1), than when it was excluded (BS 100%, BS 69% and PP 0.98; Table 1). In contrast, in analyses where the Ancylaini was recovered as monophyletic, support values for this node declined when *Canephorula* was excluded (Table 1). Interpretation of these results strongly depends on our confidence in the monophyly of the Ancylaini: if we assume that the Ancylaini are monophyletic (see below), then the inclusion of *Canephorula*, in spite of 70% of missing data for this taxon, reduced support for the "wrong" topology, namely the sister relationship between *Ancyla* and the Eucerini (as in analyses of the entire dataset), and increased the support for the "correct" topology, namely a monophyletic Ancylaini (most other analyses).

A second source of missing data in our matrix came from the fact that sequences for one of our markers, EF-1a, could not be obtained for the majority of the Eucerini. ML and Bayesian (but not MP) analyses of the molecular dataset without this gene strongly supported a monophyletic Ancylaini, indicating that EF-1a was in fact mostly responsible for the lack of monophyly for the Ancylaini (ML analyses of EF-1a alone strongly supported the grouping *Ancyla* + Eucerini, with BS values of 100%). Yet excluding a molecular partition simply because it yields unexpected result is no more appropriate than excluding some morphological characters for the same reason, unless it can be demonstrated that this partition incorporates a systematic bias into the dataset.

4.2. Saturation, rate heterogeneity and base compositional non-stationarity

In our dataset, opsin was the gene with the highest ratio of non-synonymous to synonymous substitution (0.11), and EF-1a (the gene mostly responsible for the lack of monophyly of the Ancylaini) was second (0.02). Thus, EF-1a is not an outlier in terms of tn/ts ratios and so not subject to unusual levels of saturation in relation to the other genes. Similarly, our DAMBE analyses as well as the comparison of corrected and uncorrected distances (Fig. S3b) did not suggest that EF-1a differs from the other genes regarding saturation of the third nucleotide position.

In contrast, EF-1a and NAK showed a strongly heterogeneous base composition across taxa. For EF-1a, we can pinpoint places in the tree where shifts in base composition occur: our outgroups, as well as the members of the tribes Exomalopsini, Emphorini and Tapinotaspidini, and *Tarsalia*, are either AT-rich or have equal AT to GC frequencies. In contrast, the Eucerini and *Ancyla* are markedly GC-rich (Fig. 2a). The same, but less extreme, trend is observed in NAK, although in this case *Ancyla* and the Eucerini are AT-rich (Fig. 2b). Thus the strongly supported placement of *Tarsalia* as the sister group to Eucerini + *Ancyla* in analyses of EF-1a and NAK alone (BS 100% and 61%, respectively, in ML analysis), may chiefly be due to the strikingly different base composition in these three groups. Indeed, for the third nucleotide position of EF-1a, *Tarsalia* was phenetically substantially closer (in term of corrected and uncorrected distance) to some distantly related species of Exomalopsini and Tapinotaspidini (uncorrected distances between *Tarsalia* and *Anthophorula* or *Paratetrapedia* of 0.34 and 0.35, respectively), than to *Ancyla* (uncorrected distance of 0.50). A close relationship between *Tarsalia* and either the Exomalopsini or the Tapinotaspidini is very unlikely according to the analyses of the other genes included in our study, our morphological dataset and earlier research on phylogeny of the Apinae (references in introduction).

RY-coding has been proposed to correct for biased base composition (Phillips and Penny, 2003). In addition, RY-coding strongly reduces saturation and rate heterogeneity problems, because it removes a large proportion of the silent mutations. Niehuis et al. (2012) settled the Strepsiptera enigma using only the RY-coded second position of approximately 4500 protein-coding genes. Thomas et al. (2013) reanalyzed datasets previously assembled to examine the relationships of the early winged insects and suggested that the recoding or removal of heterogeneous partitions resulted in highly resolved and consistent trees, while the non-recoded dataset failed to resolve these old relationships.

4.3. Concluding remarks on the phylogenetic position of Tarsalia and Ancyla

Of the three possible topologies between *Ancyla*, *Tarsalia* and the Eucerini, the topology inferred in parsimony analyses of the morphological dataset alone (*Ancyla* sister to *Tarsalia* + Eucerini) was recovered in none of the molecular analyses, and thus appears unlikely. Moreover, the sister relationship between *Tarsalia* and the Eucerini was supported by only two uniquely derived character states, one of them showing reversal in *Eucerinoda*, and the other associated with the mouthparts, which are strongly modified in *Ancyla*. Excluding this branching pattern leaves two possible topologies: *Tarsalia* as sister to *Ancyla* + Eucerini, and a monophyletic Ancylaini sister to the Eucerini. Forcing the first topology (*Tarsalia* sister to *Ancyla* + Eucerini) upon the morphological data for this part of the tree gives a result that is 17 steps longer than the most parsimonious tree. Characters that might support the sister group relationship between *Ancyla* and Eucerini are mostly highly homoplasious and not particularly convincing (Table S3). Forcing monophyly of the Ancylaini (ie of *Ancyla* + *Tarsalia*) results in a tree that is 9 steps longer than the most parsimonious. The characters that support a monophyletic Ancylaini are indicated in Table S3 and are also mostly homoplasious, with the exception of two unique character states: the weak apodemal ridge of the female sternum 6 (character 210; Fig. S1e) and the transverse sulcus of the male gonocoxa (263; Fig. S1d). Thus of the two alternate topologies suggested by the molecular dataset alone, parsimony analyses of the morphological dataset is less contradictory to the second, the one recovering a monophyletic Ancylaini.

Molecular data support two topologies: *Tarsalia* sister to *Ancyla* + Eucerini, and a monophyletic Ancylaini sister to the Eucerini. With the exception of parsimony analyses, the first topology was only weakly or moderately supported, whereas RY-recoding, as well as analyses without EF-1a (except parsimony analyses), strongly supported the second topology. It may be argued that the particularly high GC content of the Eucerini and of *Ancyla* in one of our markers (EF-1a) is a strong, independent synapomorphy supporting this grouping. While initial studies suggested that the GC content of homologous genes was remarkably conserved among mammals (Mouchiroud et al., 1988), growing evidence now suggests that base composition is poorly conserved phylogenetically (e.g., Betancur et al., 2013; Romiguier et al., 2010). Many studies have focused on the evolutionary forces acting on GC content of specific genomic regions (reviewed in Galtier, 2003; Romiguier et al., 2010, 2013). Galtier et al. (2001) introduced the "biased gene conversion hypothesis", which suggests that high GC-content correlates with high recombination rates: genomic regions that are subjected to high recombination rates tend to see their GC-content increase due to GC-biased DNA-repair mechanisms. The factors influencing the distribution of recombination in the genome have also received much attention. In addition to broad scale factors such as distance to telomere, small-scale "recombination hotspots" have also been recognized (references in Lartillot, 2013). While broad-scale factors tend to be phylogenetically conserved, small-scale hotspots are highly variable among and even within species (reviewed in Lartillot, 2013). Consequently, no evidence enables us to postulate that the high GC-content in one of the markers included in our study may be indicative of true phylogenetic relationships. In our dataset, base composition of EF-1a and NAK was not particularly conserved phylogenetically. Indeed, two eucerine genera, *Florilegus* and *Svastrina,* that formed a well-supported monophyletic groups in all analyses (including morphology) have a divergent base composition in the third nucleotide position of NAK (57% and 67% respectively) despite diverging only ~12 mya (Fig. 4); this divergence (a difference of 10% over 12 mya) is comparatively larger than the divergence observed between *Tarsalia* and *Ancyla* (6% for the third position of NAK and 23% for the third position of EF-1a over 45 my).

We therefore conclude that the most convincing interpretation of the entire data we have amalgamated is that the Ancylaini is a monophyletic group. Further testing of this hypothesis with additional markers, e. g., in a phylogenomic study, is highly desirable. More generally, we recommend testing for homogeneity of base composition in any phylogenetic study, and to systematically conduct multiple phylogenetic analyses of a matrix where heterogeneous partitions have been recoded or excluded. Such analyses will readily highlight systematic errors caused by non-stationarity. In the most recent higher-level phylogenetic dataset for bees (Cardinal and Danforth, 2013), the third position of each gene was significantly heterogeneous (data not shown); the third position of NAK (a widely used marker in bee phylogenetics) is heretogeneous in most published bee datasets (e.g., Cardinal et al., 2010; Kawakita et al., 2008; Litman et al., 2011; Payne, 2014; Praz et al., 2008). With one exception (the amino acid dataset was analyzed in Kawakita et al. (2008), resulting in weakly supported trees) the influence of this bias remains untested.

4.4. Biogeography

The argument that the Ancylaini constitutes a monophyletic group also implies the most parsimonious biogeographic scenario, as it involves only one ancient (between 69 and 47 mya) geodispersal event from the New World to the Old World. In the period between 47 mya and 22 mya, no exchange between eastern and western hemispheres is indicated in our analyses. However, after 22 mya, at least three geodispersal events occurred among the genera *Tetralonia, Tetraloniella* and *Eucera* (probably more if multiple

lineages of the diverse genera *Tetraloniella* and *Eucera* or the ancestor of *Notolonia* migrated separately).

Geodispersal requires both a plausible route and suitable environmental conditions. The two main routes available at the relevant time period are the Bering Land Bridge (BLB) and one of several possible North Atlantic Land Bridges (NALB). The most important of the latter was the Thulean Bridge, which united Eastern North America and Europe through what are now Greenland, Iceland, Faroe Islands and Scotland. The De Geer Bridge connected the Canadian Arctic Archipelago to Fennoscandia through northern Greenland but was isolated from most of Europe as a result of the Danish–Polish trough (Sanmartín et al., 2001). The BLB was available throughout the relevant time period for the Ancylaini, 69–47 mya, while all NALBs were likely interrupted by 50 mya (Condamine et al., 2013; Ren et al., 2013; Sanmartín et al., 2001) although more recent geodispersal over narrow straits of the Northern Atlantic, but not necessarily over a continuous land bridge, have been suggested (Davis et al., 2002, 2004; Denk et al., 2010). Of these options, the Thulean Bridge is considered the most likely for two main reasons. First it is further south and thus had a warmer climate (see below). Second, it connected Eastern North America with the main body of the Western Palaearctic where both genera of Ancylaini primarily occur (see Introduction). If the Ancylaini got to the Western Palaearctic via the BLB they would have had to cross the Turgai Strait that united the Tethys and Arctic Oceans from 180 to 30 mya (Rose, 2012; Sanmartín et al., 2001; Tiffney, 1985. Pereda-Suberbiola et al., 2009 suggest a later origin of the Turgai Strait, but still well before our estimated MRCA for the Ancylaini). The importance of the Turgai Strait as a barrier to geodispersal is debated. Corbiculate bees traversed it as several genera are found in both Baltic and Cambay amber (Engel et al., 2013) and various mammals dispersed from one side of the strait to the other (Rose, 2012; Vislobokova, 2013). Conversely, the Turgai Strait was a complete barrier to the plant genus *Decodon*, even though its seeds are dispersed by aquatic birds (Grímsson et al., 2012). Other taxa which have been considered to have used the NALB to move from North America to the Palaearctic at a time that brackets those considered for the Ancylaini include Malphigiaceae (Davis et al., 2002, 2004), Bufonidae (Pramuk et al., 2008), Crocodyloidea (Puértolas et al., 2011), Alligatoroidea (Martin and Lauprasert, 2010), hadrosaurs (Pereda-Suberbiola et al., 2009) and both marsupial (Martin et al., 2005; but see Vullo et al., 2009) and placental (Solé and Smith, 2013) mammals. Insect taxa for which similarly timed geodispersal have been demonstrated include giant ants (Archibald et al., 2011) and melanopline grasshoppers (Chintauan-Marquier et al., 2014). Cruaud et al. (2012) posited the geodispersal of the ancestors of a modern genus of figs and its fig wasp pollinators from Eurasia to the New World across a NALB at a time period that overlaps with the earlier estimates we have for the geodispersal of Ancylaini, but in the opposite direction. Conversely, Martin and Lauprasert (2010) and Chintauan-Marquier et al. (2014) had some examples supporting the BLB route and Townsend et al. (2011) argued for this route for dibamid squamates.

As for environmental conditions, lineages such as *Tarsalia*, *Ancyla*, early branches in the Eucerini, as well as the vast majority of the non-eucerine lineages of the eucerine line (except a few species of *Exomalopsis* and of *Diadasia*), are nowadays restricted to megathermal areas with a mean annual temperature (MAT) above 15 °C (at least 13 °C for the known localities for *Eucerinoda*; see below for discussion of more cold tolerant Eucerina).

Conditions suitable for thermophilic organisms existed in the arctic at various times during the early Eocene, all between 56 and 50 mya (Eberle and Greenwood, 2012; Zachos et al., 2008). The first, the PETM, occurred at the Paleocene/Eocene boundary 55 mya, but was very short-lived, lasting perhaps 170 kyr. The second occurred around 53.5 mya and was also short-lived. In contrast, the Early Eocene Climatic Optimum (EECO) lasted approximately two million years ending approximately 50 mya. Clearly dating particular geodispersal events among such tightly clustered warm periods is problematic (although Solé and Smith (2013) argued for the very brief PETM for some placental carnivores).

Archibald et al. (2011) marshal evidence for strong warming in the arctic sufficient to permit a highly thermophilic, giant formicine ant to migrate from the Old World to the New. They note that the largest modern ants are found in areas where MAT is at least 17 °C and generally above 20 °C and note that early to middle Eocene floras from Greenland and Axel Heiberg Island had MAT estimates of 12–16 °C, which, while insufficient for giant ants, should certainly have been suitable for an ancestor of extant Ancylaini. Consequently, we suggest that the ancestor to the Ancylaini reached the Old World from the New World across the Thulean Land Bridge, likely at some point between 67 and 50 mya, but probably during the last hypsithermal event that occurred just before this bridge was interrupted around 50 mya.

The more cold-adapted eucerine genera: *Tetralonia, Tetraloniella* and *Eucera* moved between the Old and New Worlds less than 22 mya. Some species of these genera, and their relative *Peponapis,* inhabit areas with a MAT as low as 5 °C. The BLB may be the most likely route for these events because it was uninterrupted from 20 to 8 mya (Milne, 2006) and it hosted a warm-temperate deciduous forest during the Early Miocene (Wolfe, 1994; Wolfe and Leopold, 1967).

In conclusion, our data suggest that two distinct routes between North America and the Palaearctic may have facilitated exchanges of different biotic faunal elements during different times: warm-adapted lineages may have used the NALB during the Eocene, while exchanges in more temperate lineages were possible later over the Bering Land Bridge. There may have been several migration routes explaining the current distribution of most bee lineages in both eastern and western hemispheres. Litman et al. (2011) suggested a Cretaceous, Gondwanan vicariance for basal Megachilidae; Almeida et al. (2012) demonstrated frequent exchanges between Australia and South America through Antarctica in colletid bees in the time window comprised between 70 and 30 mya; several studies have suggested faunal exchanges through the Bering Land Bridge (e.g., Hines, 2008; Praz et al., 2008; Rehan et al., 2010; Sedivy et al., 2013). Our study is the first to suggest faunal exchange over the North Atlantic Land Bridge in bees, in spite of the documented importance of this route for other organisms.

Acknowledgments

The junior author's fieldwork in Chile has been supported by the Natural Sciences and Engineering Research Council of Canada, the National Geographic Society and his own salary. The imaging system used for figures S1 was obtained with funds from the Canadian Foundation for Innovation and the Ontario Research Fund through Canadensys. Molecular work was funded by the University of Neuchâtel and greatly facilitated by the team of the Genetic Diversity Center of ETH Zurich. We thank Sheila Dumesh for taking the images, Claudio Sedivy and Alireza Monfared for making a field trip to Iran possible, and the various collectors and taxonomists named in Table S1 for specimens and identifications. CP also thanks Julien Vieu for help with the biogeographic analyses and Thomas Degen for assistance with figure preparation. We thank Jessica Litman, two anonymous reviewers and the subject editor for useful comments on the manuscript.

Appendix A. Supplementary material

Supplementary data associated with this article can be found, in the online version, at http://dx.doi.org/10.1016/j.ympev.2014.09.003.

References

Alexander, B.A., Michener, C.D., 1995. Phylogenetic studies of the families of short-tongued bees. Univ. Kans. Sci. Bull. 55, 377–424.

Almeida, E.A.B., Danforth, B.N., 2009. Phylogeny of colletid bees (Hymenoptera: Colletidae) inferred from four nuclear genes. Mol. Phylogenet. Evol. 50, 290–309.

Almeida, E.A.B., Pie, M.R., Brady, S.G., Danforth, B.N., 2012. Biogeography and diversification of colletid bees (Hymenoptera: Colletidae): emerging patterns from the southern end of the world. J. Biogeogr. 39, 526–544.

Archibald, S.B., Johnson, K.R., Mathewes, R.W., Greenwood, D.R., 2011. Intercontinental dispersal of giant thermophilic ants across the Arctic during early Eocene hyperthermals. Proc. R. Soc. B 278, 3679–3686.

Ascher, J.S., Pickering, J., 2014. Discover Life Bee Species Guide and World Checklist (Hymenoptera: Apoidea: Anthophila). <http://www.discoverlife.org/mp/20q?guide=Apoidea_species>.

Baker, D.B., 1998. Taxonomic and phylogenetic problems in Old World eucerine bees with special reference to the genus *Tarsalia* Morawitz, 1895 (Hymenoptera: Apoidea: Anthophoridae). J. Nat. Hist. 32, 823–860.

Betancur-R., R., Li, C., Munroe, T.A., Ballesteros, J.A., Ortí, G., 2013. Addressing gene tree discordance and non-stationarity to resolve a multi-locus phylogeny of the flatfishes (Teleostei: Pleuronectiformes). Syst. Biol. 62, 763–785.

Cardinal, S., Danforth, B.N., 2013. Bees diversified in the age of eudicots. Proc. R. Soc. B 280, 20122686.

Cardinal, S., Straka, J., Danforth, B.N., 2010. Comprehensive phylogeny of apid bees reveals the evolutionary origins and antiquity of cleptoparasitism. Proc. Natl. Acad. Sci. USA 107, 16207–16211.

Carpenter, J.M., 1988. Choosing among multiple equally parsimonious cladograms. Cladistics 8, 147–153.

Chintauan-Marquier, I.C., Amédégnato, C., Nichols, R.A., Pompanon, F., Grandcolas, P., Desutter-Grandcolas, L., 2014. Inside the Melanoplinae: new molecular evidence for the evolutionary history of the Eurasian Podismini (Orthoptera: Acrididae). Mol. Phylogenet. Evol. 71, 224–733.

Condamine, F.L., Sperling, F.A.H., Kergoat, G.J., 2013. Global biogeographical pattern of swallowtail diversification demonstrates alternative colonization routes in the Northern and Southern hemispheres. J. Biogeogr. 40, 9–23.

Crawley, S.S., Hilu, K.W., 2012. Impact of missing data, gene choice, and taxon sampling on phylogenetic reconstruction: the Caryophyllales (angiosperms). Plant. Syst. Evol. 298, 297–312.

Cruaud, A., Rønsted, N., Chantarasuwan, B., Chou, L.S., Clement, W., Couloux, A., Cousins, B., Forest, F., Genson, G., Harrison, R.D., Hossaert-McKey, M., Jabbour-Zahab, R., Jousselin, E., Kerdelhué, C., Kjellberg, F., Lopez-Vaamonde, C., Peebles, J., Pereira, R.A.S., Schramm, T., Ubaidillah, R., van Noort, S., Weiblen, G.D., Yang, D.R., Yan-Qiong, P., Yodpinyanee, A., Libeskind-Hadas, R., Cook, J.M., Rasplus, J.Y., Savolainen, V., 2012. An extreme case of plant-insect co-diversification: figs and fig-pollinating wasps. Syst. Biol. 61, 1029–1047.

Danforth, B.N., Brady, S.G., Sipes, S.D., Pearson, A., 2004. Single-copy nuclear genes recover Cretaceous-age divergences in bees. Syst. Biol. 53, 309–326.

Danforth, B.N., Cardinal, S., Praz, C., Almeida, E.A.B., Michez, D., 2013. The impact of molecular data on our understanding of bee phylogeny and evolution. Annu. Rev. Entomol. 58, 57–78.

Danforth, B.N., Ji, S., 1998. Elongation factor-1α occurs as two copies in bees: implications for phylogenetic analysis of EF-1α in insects. Mol. Biol. Evol. 15, 225–235.

Danforth, B.N., Sipes, S., Fang, J., Brady, S.G., 2006. The history of early bee diversification based on five genes plus morphology. Proc. Natl. Acad. Sci. USA 103, 15118–15123.

Davis, C.C., Bell, C.D., Mathews, S., Donoghue, M.J., 2002. Laurasian migration explains Gondwanan disjunctions: evidence from Malpighiaceae. Proc. Natl. Acad. Sci. 99, 6833–6837.

Davis, C.C., Fritsch, P.W., Bell, C.D., Mathews, S., 2004. High-latitude tertiary migrations of an exclusively tropical clade: evidence from Malpighiaceae. Int. J. Plant Sci. 165, S107–S121.

Denk, T., Grímsson, F., Zetter, R., 2010. Episodic migration of oaks to Iceland: evidence for a North Atlantic "land bridge" in the latest Miocene. Am. J. Bot. 97, 276–287.

Drummond, A.J., Suchard, M.A., Xie, D., Rambaut, A., 2012. Bayesian phylogenetics with BEAUti and the BEAST 1.7. Mol. Biol. Evol. 29, 1969–1973.

Eberle, J.J., Greenwood, D.R., 2012. Life at the top of the greenhouse Eocene world – a review of the Eocene flora and vertebrate fauna from Canada's High Arctic. GSA Bull. 124, 3–23.

Engel, M.S., Ortega-Blanco, J., Nascimbene, P.C., Singh, H., 2013. The bees of Early Eocene Cambay amber. J. Melittol. 25, 1–12.

Farris, J.J., 1969. A successive approximations approach to character weighting. Syst. Biol. 18, 374–385.

Galtier, N., 2003. Gene conversion drives GC content evolution in mammalian histones. Trends Genet. 19, 65–68.

Goloboff, P. 1999. NONA ver. 2. Published by the author, Tucumán, Argentina.

Galtier, N., Piganeau, G., Mouchiroud, D., Duret, L., 2001. GC-content evolution in mammalian genomes: the biased gene conversion hypothesis. Genetics 159, 907–911.

Goloboff, P.A., Farris, J.S., Källersjö, M., Oxelman, B., Ramírez, M.J., Szumik, C.A., 2003. Improvements to resampling measures of group support. Cladistics 19, 324–332.

Goloboff, P.A., Farris, J.S., Nixon, K.C., 2008. TNT, a free program for phylogenetic analysis. Cladistics 24, 774–786.

Gonzalez, V.H., Griswold, T., Engel, M.S., 2013. Obtaining a better taxonomic understanding of native bees: where do we start? Syst. Entomol. 38, 645–653.

Gonzalez, V.H., Griswold, T., Praz, C.J., Danforth, B.N., 2012. Phylogeny of the bee family Megachilidae (Hymenoptera: Apoidea) based on adult morphology. Syst. Entomol. 37, 261–286.

Grímsson, F., Ferguson, D.K., Zetter, R., 2012. Morphological trends in the fossil pollen of *Decodon* and the paleobiogeographic history of the genus. Int. J. Plant Sci. 173, 297–317.

Hines, H.M., 2008. Historical biogeography, divergence times, and diversification patterns of bumble bees (Hymenoptera: Apidae: *Bombus*). Syst. Biol. 57, 58–75.

Hovmöller, R., Knowles, L.L., Kubatko, L.S., 2013. Effects of missing data on species tree estimation under the coalescent. Mol. Phylogenet. Evol. 69, 1057–1062.

Huelsenbeck, J.P., Ronquist, F., 2001. MRBAYES: Bayesian inference of phylogeny. Bioinformatics 17, 754–755.

Katoh, K., Misawa, K., Kuma, K.I., Miyata, T., 2002. MAFFT: a novel method for rapid multiple sequence alignment based on fast Fourier transform. Nucl. Acids Res. 30, 3059–3066.

Kawakita, A., Ascher, J.S., Sota, T., Kato, M., Roubik, D.W., 2008. Phylogenetic analysis of the corbiculate bee tribes based on 12 nuclear protein-coding genes (Hymenoptera: Apoidea: Apidae). Apidologie 39, 163–175.

Lanfear, R., Calcott, B., Ho, S.Y.W., Guindon, S., 2012. PartitionFinder: combined selection of partitioning schemes and substitution models for phylogenetic analyses. Mol. Biol. Evol. 29, 1695–1701.

Lartillot, N., 2013. Phylogenetic patterns of GC-biased gene conversion in placental mammals and the evolutionary dynamics of recombination landscapes. Mol. Biol. Evol. 30, 489–502.

Lemmon, A.R., Brown, J.M., Stanger-Hall, K., Moriarty Lemmon, E., 2009. The effect of ambiguous data on phylogenetic estimates obtained by maximum likelihood and Bayesian inference. Syst. Biol. 58, 130–145.

Litman, J., Danforth, B.N., Eardley, C.D., Praz, C.J., 2011. Why do leafcutter bees cut leaves? New insights into the early evolution of bees. Proc. R. Soc. B 278, 3593–3600.

Lockhart, P.J., Cameron, S.A., 2001. Trees for bees. Trends Ecol. Evol. 16, 84–88.

Maddison, D.R., Maddison, W.P., 2005. Macclade 4.08 for OSX. Sinauer Associates Inc, Sunderland, Massachusetts.

Martin, J.E., Case, J.A., Jagt, J.W.M., Schulp, A.S., Mulder, E.W.A., 2005. A new European marsupial indicates a Late Cretaceous high-latitude Transatlantic dispersal route. J. Mamm. Evol. 12, 495–511.

Martin, J.E., Lauprasert, K., 2010. A new primitive alligatorine from the Eocene of Thailand: relevance of Asiatic members to the radiation of the group. Zool. J. Linn. Soc. 158, 608–628.

Matzke, N.J., 2013. Probabilistic Historical Biogeography: New Models for Founder-Event Speciation, Imperfect Detection, and Fossils Allow Improved Accuracy and Model-Testing. Ph.D. thesis, Department Integrative Biology and Designated Emphasis in Computational and Genomic Biology, University of California, Berkeley, pp. 1–240.

Michener, C.D., 2007. The Bees of the World, second ed. The Johns Hopkins University Press, Baltimore.

Michez, D., Vanderplanck, M., Engel, M.S., 2011. Fossil bees and their plant associates. In: Patiny, S. (Ed.), Evolution of Plant-Pollinator Relationships. Cambridge University Press, Cambridge, pp. 103–164.

Milne, R.I., 2006. Northern Hemisphere plant disjunctions: a window on tertiary land bridges and climate change? Ann. Bot. 98, 465–472.

Mouchiroud, D., Gautier, C., Bernardi, G., 1988. The compositional distribution of coding sequences and DNA molecules in humans and murids. J. Mol. Evol. 27, 311–320.

Niehuis, O., Hartig, G., Grath, S., Pohl, H., Lehmann, J., Tafer, H., Donath, A., Krauss, V., Eisenhardt, C., Hertel, J., Petersen, M., Mayer, C., Meusemann, K., Peters, R.S., Stadler, P.F., Beutel, R.G., Bornberg-Bauer, E., McKenna, D.D., Misof, B., 2012. Genomic and morphological evidence converge to resolve the enigma of Strepsiptera. Curr. Biol. 22, 1–5.

Nixon, K.C., 1999. The parsimony ratchet, a new method for rapid parsimony analysis. Cladistics 15, 407–414.

Nixon, K.C., 2004. ASADO Version 1.7. Made available through the author. Cornell University, Ithaca, New York, United States of America.

Pagel, M., 1999. The maximum likelihood approach to reconstructing ancestral character states of discrete characters on phylogenies. Syst. Biol. 48, 612–622.

Paradis, E., Claude, J., Strimmer, K., 2004. APE: analyses of phylogenetics and evolution in R language. Bioinformatics 20, 289–290.

Payne, A., 2014. Resolving the relationships of apid bees (Hymenoptera: Apidae) through a direct optimization sensitivity analysis of molecular, morphological, and behavioural characters. Cladistics 30, 11–25.

Pereda-Suberbiola, X., Canudo, J.I., Cruzado-Caballero, P., Barco, J.L., López-Martínez, N., Oms, O., Ruiz-Omeñaca, J.I., 2009. The last hadrosaurid dinosaurs of Europe: a new lambeosaurine from the Uppermost Cretaceous of Aren (Huesca, Spain). Compt. Rend. Palevol 8, 559–572.

Phillips, M.J., Penny, D., 2003. The root of the mammalian tree inferred from whole mitochondrial genomes. Mol. Phylogenet. Evol. 28, 171–185.

Pramuk, J.B., Robertson, T., Sites, J.W., Noonan, B.P., 2008. Around the world in 10 million years: biogeography of the nearly cosmopolitan true toads (Anura: Bufonidae). Global Ecol. Biogeogr. 17, 72–83.
Praz, C.J., Müller, A., Danforth, B.N., Griswold, T.L., Widmer, A., Dorn, S., 2008. Phylogeny and biogeography of bees of the tribe Osmiini (Hymenoptera: Megachilidae). Mol. Phylogenet. Evol. 49, 185–197.
Puértolas, E., Canudo, J.I., Cruzado-Caballero, P., 2011. A new crocodylian from the Late Maastrichtian of Spain: implications for the initial radiation of crocodyloids. PLoSOne 6, e20011.
R Core Team, 2014. R: A Language and Environment for Statistical Computing. R Foundation for Statistical Computing, Vienna, Austria. <http://www.R-project.org>.
Rambaut, A. 2012. FigTree v.1.3.1.1. <http://tree.bio.ed.ac.uk/software/figtree/>.
Rambaut, A., Suchard, M.A., Xie, D., Drummond, A.J., 2014. Tracer v1.6. <http://beast.bio.ed.ac.uk/Tracer>.
Ree, R., Smith, S., 2008. Maximum likelihood inference of geographic range evolution by dispersal, local extinction, and cladogenesis. Syst. Biol. 57, 4–14.
Rehan, S.R., Chapman, T.W., Craigie, A.I., Richards, M.H., Cooper, S.J.B., Schwarz, M.P., 2010. Molecular phylogeny of the small carpenter bees (Hymenoptera: Apidae: Ceratinini) indicates early and rapid global dispersal. Mol. Phylogenet. Evol. 55, 1042–1054.
Ren, Z., Zhong, Y., Kurosu, U., Aoki, S., Ma, E., von Dohlen, C.D., Wen, J., 2013. Historical biogeography of Eastern Asian-Eastern North American disjunct Melaphidina aphids (Hemiptera: Aphididae: Eriosomatinae) on Rhus hosts (Anacardiaceae). Mol. Phylogenet. Evol. 69, 1146–1158.
Roig-Alsina, A., Michener, C.D., 1993. Studies of the phylogeny and classification of long-tongued bees (Hymenoptera: Apoidea). Univ. Kans. Sci. Bull. 55, 123–162.
Romiguier, J., Ranwez, V., Delsuc, F., Galtier, N., Douzery, E.J.P., 2013. Less is more in mammalian phylogenomics: AT-rich genes minimize tree conflicts and unravel the root of placental mammals. Mol. Biol. Evol. 30, 2134–2144.
Romiguier, J., Ranwez, V., Douzery, E.J.P., Galtier, N., 2010. Contrasting GC-content dynamics across 33 mammalian genomes: relationship with life-history traits and chromosome sizes. Genome Res. 20, 1001–1009.
Ronquist, F., Huelsenbeck, J.P., 2003. MRBAYES 3: Bayesian phylogenetic inference under mixed models. Bioinformatics 19, 1572–1574.
Rose, K.D., 2012. The importance of Messel for interpreting Eocene Holarctic mammalian faunas. Palaeobio. Palaeoenv. 92, 631–647.
Roure, B., Baurain, D., Philippe, H., 2012. Impact of missing data on phylogenies inferred from empirical phylogenomic data sets. Mol. Biol. Evol. 30, 197–214.
Sanmartín, I., Enghoff, H., Ronquist, F., 2001. Patterns of animal dispersal, vicariance and diversification in the Holarctic. Biol. J. Linn. Soc. 73, 345–390.
Sedivy, C., Dorn, S., Müller, A., 2013. Molecular phylogeny of the bee genus *Hoplitis* (Megachilidae: Osmiini) – how does nesting biology affect biogeography? Zool. J. Linn. Soc. 167, 28–42.
Silveira, F.A., 1993a. Phylogenetic relationships of the Exomalopsini and Ancylini (Hymenoptera: Apidae). Univ. Kans. Sci. Bull. 55, 163–173.
Silveira, F.A., 1993b. The mouthparts of *Ancyla* and the reduction of the labiomaxillary complex among long-tongued bees. Ent. Scand. 24, 293–300.
Silveira, F.A., 1995. Phylogenetic relationships and classification of Exomalopsini with a new tribe Teratognathini (Hymenoptera: Apoidea). Univ. Kans. Sci. Bull. 55, 425–454.
Solé, F., Smith, T., 2013. Dispersals of placental carnivorous mammals (Carnivoramorpha, Oxyaenodonta & Hyaenodontida) near the Paleocene-Eocene boundary: a climatic and almost worldwide story. Geol. Belg. 16, 254–261.
Spaethe, J., Briscoe, A.D., 2004. Early duplication and functional diversification of the opsin gene family in insects. Mol. Biol. Evol. 21, 1583–1594.
Stamatakis, A., Ludwig, T., Meier, H., 2005. RAxML-III: a fast program for maximum likelihood-based inference of large phylogenetic trees. Bioinformatics 21, 456–463.
Straka, J., Bogusch, P., 2007. Phylogeny of the bees of the family Apidae based on larval characters with focus on the origin of cleptoparasitism (Hymenoptera: Apiformes). Syst. Entomol. 32, 700–711.
Straka, J., Rozen, J.G., 2012. First observations on nesting and immatures of the bee genus *Ancyla* (Apoidea: Apidae: Apinae: Ancylaini). Am. Mus. Novit. 3749, 1–24.
Swofford, D.L., 2002. Paup. 4.0b10 for Macintosh. Sinauer Associates Inc, Sunderland, Massachusetts.
Tamura, K., Peterson, D., Peterson, N., Stecher, G., Nei, M., Kumar, S., 2011. MEGA5: Molecular evolutionary genetics analysis using maximum likelihood, evolutionary distance, and maximum parsimony methods. Mol. Biol. Evol. 28, 2731–2739.
Thomas, J.A., Trueman, J.W.H., Rambaut, A., Welch, J.J., 2013. Relaxed phylogenetics and the Palaeoptera problem: resolving deep ancestral splits in the insect phylogeny. Syst. Biol. 62, 285–297.
Tiffney, B.H., 1985. The Eocene North Atlantic land bridge: its importance in Tertiary and modern phytogeography of the Northern Hemisphere. J. Arnold Arbor. 66, 243–273.
Townsend, T.M., Leavitt, D.H., Reeder, T.W., 2011. Intercontinental dispersal by a microendemic burrowing reptile (Dibamidae). Proc. R. Soc. B 278, 2568–2574.
Upchurch, P., 2008. Gondwanan break-up: legacies of a lost world? Trends Ecol. Evol. 23, 229–236.
Vislobokova, I.A., 2013. Ecological evolution of Early Cetartiodactyla and reconstruction of its missing initial link. Paleontol. J. 47, 533–548.
Vivallo, F., 2010. Notes on the bee genus *Alloscirtetica* Holmberg, 1909 in northern Chile with the description of two new altiplanic species and a key for the Chilean species of Eucerini (Hymenoptera: Apidae). Zootaxa 2010, 16–30.
Vullo, R., Gheerbrant, E., de Muizon, C., Néraudeau, D., 2009. The oldest modern therian mammal from Europe and its bearing on stem marsupial paleobiogeography. Proc. Natl. Acad. Sci. USA 106, 19910–19915.
Warncke, K., 1979. Beitrag zur Bienenfauna des Iran: 10. Die Gattung *Ancyla* Lep., mit einer Revision der Bienengattung *Ancyla* Lep. Bol. Mus. Civ. Venezia 30, 183–195.
Wiens, J.J., Morill, M.C., 2011. Missing data in phylogenetic analysis: reconciling results from simulations and empirical data. Syst. Biol. 60, 719–731.
Wiens, J.J., Tiu, J., 2012. Highly incomplete taxa can rescue phylogenetic analyses from the negative impacts of limited taxon sampling. PloSOne 7, e42925.
Wolfe, J.A., 1994. An analysis of Neogene climates in Beringia. Palaeogeogr. Palaeoclim. Palaeoecol. 108, 207–216.
Wolfe, J.A., Leopold, E.B., 1967. Neogene and Early Quaternary vegetation of northwestern North America and northeastern Asia. In: Hopkins, D.M. (Ed.), The Bering Land Bridge. Stanford University Press, Stanford, pp. 193–206.
Xia, X., 2013. DAMBE5: A comprehensive software package for data analysis in molecular biology and evolution. Mol. Biol. Evol. 30, 1720–1728.
Xia, X., Lemey, P., 2009. Assessing substitution saturation with DAMBE. In: Lemey, P., Salemi, M., Vandamme, A.-M. (Eds.), The Phylogenetic Handbook: A Practical Approach to Phylogenetic Analysis And Hypothesis Testing. Cambridge University Press, Cambridge, pp. 615–630.
Xia, X., Xie, Z., Salemi, M., Chen, L., Wang, Y., 2003. An index of substitution saturation and its application. Mol. Phylogenet. Evol. 26, 1–7.
Xu, B., Yang, Z., 2013. PAMLX: a graphical user interface for PAML. Mol. Biol. Evol. 30, 2723–2724.
Yang, Z., Nielsen, R., 2000. Estimating synonymous and nonsynonymous substitution rates under realistic evolutionary models. Mol. Biol. Evol. 17, 32–43.
Zachos, J.C., Dickens, G.R., Zeebe, R.E., 2008. An early Cenozoic perspective on greenhouse warming and carbon-cycle dynamics. Nature 451, 279–283.